CFD Simulation of High Inlet Velocity Air Flow into a Large Tank at Pool Scrubbing Conditions

Erol Bicer [a,b*], Hyoung Kyu Cho[b], Hong Soon Joon[a]
[a]*FNC Tech., Heungdeok IT Valley, Heungdeok 1-ro, Giheung-gu, Yongin-si, Gyeonggi-do, 446-908, Korea*
[b]*Department of Nuclear Engineering, Seoul National Univ., 1 Gwanak-ro, Gwanak-gu, Seoul 08826*
[*]*Corresponding author: ebicer@fnctech.com*

1. Introduction

According to TEPCO Progress Report No.4 [1], the post-radiation measurements after the Fukushima Daiichi nuclear disaster revealed that the fission product retention was less effective than it was previously predicted. Thus, the pool scrubbing phenomenon was brought back on the spotlights again in the nuclear safety community since it enables the reduction of source terms to the environment in the event of hypothetical severe accidents.

Pool scrubbing is the removal of the airborne fission products in gas bubbles rising in a large body of water, i.e., a water pool. Originally, pool scrubbing was related to suppression pools in BWRs however, the phenomenon also occurs in the steam generators of PWRs. The removal effect (retention capacity) of the radioactive aerosol is quantified by the so-called Decontamination Factor (DF) which is defined as the quotient between the mass injected and the mass escape from the pool.

The separate effect tests that were performed in the past have shown that the DF is dependent on many parameters such as particle size and concentration, bubble size and distribution, submergence, pool depth, pool P/T (pressure and temperature), gas composition, and so on. Especially, the bubble size and shape play a very crucial role in the retention capacity. Thus, it's important to understand the hydrodynamic behavior of the pool scrubbing phenomenon well through numerical simulations using CFD.

2. Methods and Results

Pool scrubbing is characterized by three main areas; hydrodynamics, thermohydraulics, and aerosol removal. Since the main concern is the stable bubble size and shape, the area of hydrodynamics will be discussed more in detail throughout this paper.

2.1 Bubble Behavior

The large bubbles (globules) exiting the vent disperses into a swarm of smaller bubbles within a few globule diameters of the vent. Depending on the inlet gas flow rate and the submergence, the swarm rises to the pool surface quickly due to the increase of gas volume caused by the decrease of static pressure. Most of the bubbles are collapsed and entrained into the atmosphere once they reach the surface. The behavior is shown in Fig. 1 below. The bubble size in the swarm region is considered constant due to immense bubble interactions. The recent experiments [2] have shown that the stable bubble size distribution in the swarm region is essentially lognormal and this distribution plays an important role in estimating an accurate DF.

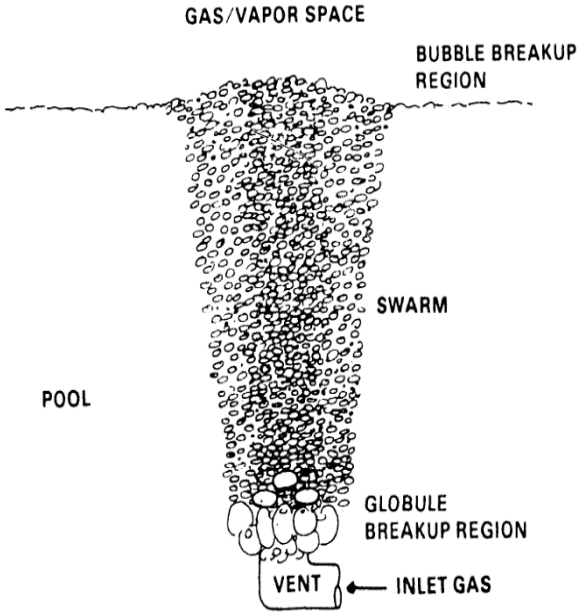

Fig. 1. Bubble behavior during pool scrubbing [3]

2.2 Pool Scrubbing Geometry and Flow Regimes

Flow patterns two-phase flow in water pools, large and small-diameter pipes are inherently different from each other. In nuclear engineering, a long small-diameter pipe is commonly used in experiments and theoretical studies due to the assumption of a developed flow in high L/D aspect ratios and there is no distinct or quantitative differentiation between a pipe and a pool.

Generally, bubbly and churn-turbulent flow regimes are observed in these large diameters and slug flow cannot be sustained due to the large diameter. In the case of the annular flow, it does not occur in water pools due to the absence of confining walls. Usually, further increasing the gas flow rate would result in a droplet flow regime. However, these kinds of hyper velocities are not common in industrial applications. Thus, the concerned flow patterns for two-phase flow in a liquid pool are bubbly and churn-turbulent flows. Considering all of the above, Y. Abe et. al. [2] experiment is chosen to be studied in this paper

2.3 Pool Scrubbing Experiment

A recent experiment was conducted by Y. Abe et. al. [2] to study the flow structures of the gas-phase jet in pool scrubbing. In the experiment, the air was injected through a 6 mm inner-diameter nozzle into a rectangular test section (500×500×3000 mm) that was filled up 1100 mm with tap water at room temperature.

Along the flow direction, the measurements were taken at five different elevations (h=100, 300, 500, 700, and 900 mm). The void fraction, gas velocity, and the bubble size distribution are reported (Fig. 2.) for one case in which the Weber number is in the order of 10^6. In this case, the inlet superficial velocity (J_g) is around 150 m/s which is quite high compared to similar experiments in the literature. The details of the experiment can be found at Y. Abe et. al. [2].

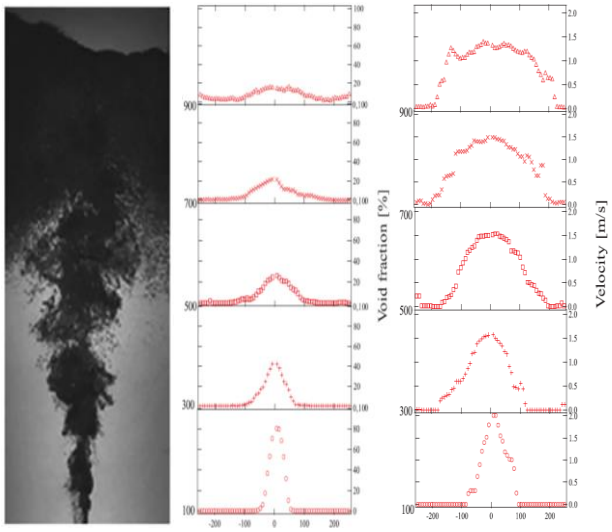

Fig. 2. Y. Abe et. al. [2] experiment results for J_g =150 m/s

2.4 OpenFOAM Model

OPEN source Field Operation And Manipulation (OpenFOAM) is a free and open-source CFD toolbox that is widely used in academia and industry to solve with a huge solver database. The *multiphaseEulerFoam* solver, which is a solver for a system of any number of compressible fluid phases with a common pressure but otherwise separate properties, was selected to simulate the Y. Abe et. al. [2] experiment in OpenFOAM. This solver is commonly used when simulating two-fluid phases with one phase dispersed in another, i.e., air and water. Since both of the phases are described using the Eulerian conservation equations and it is referred to as the Euler-Euler model.

In the model, both phases are viewed as interacting and interpenetrating continua which are coupled by the mass, momentum, and energy transfer terms between them. Assuming an incompressible two-phase flow with no phase change, equations (1) and (2) have to be solved for both cases. $\alpha_k, \bar{u}_k$ and $\bar{R}_k^{eff}$ stands for volumetric phase fraction, phase velocity, and effective Reynold's stress tensor, respectively.

$$\frac{\partial \alpha_k}{\partial t} = \nabla.(\alpha_k.\bar{u}_k) = 0 \tag{1}$$

$$\frac{\partial(\alpha_k.u_k)}{\partial t} + \nabla.(\alpha_k\bar{u}_k\bar{u}_k) + \nabla.\left(\alpha_k\bar{R}_k^{eff}\right) = \frac{\alpha_k}{\bar{\rho}_k}\nabla\bar{P} + \alpha_k g + \frac{\sum F_i}{\bar{\rho}_k} \tag{2}$$

The averaging process in the equations leads to unresolved flow structure which can be compensated by modeling the phase interaction terms represented by $\sum F_i$. However, the closure modeling mainly relies on the empirical correlations therefore it is greatly flow regime and properties dependent. $\sum F_i$ represents the sum of all interfacial forces which also takes into account the momentum transfer between the phases. In OpenFOAM, these terms can be activated in the *constant/phaseProperties* file and the available models are shown in Fig 3. below.

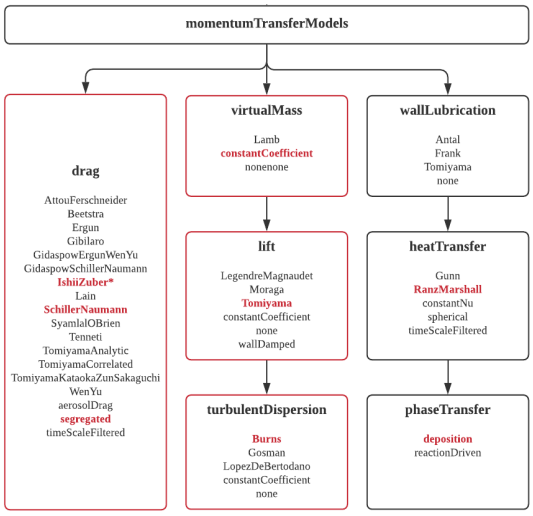

Fig. 3. OpenFOAM phase interaction models

Based on a literature survey to obtain a stable swarm in high-velocity airflow cases, the following forces were found to be the most important ones; the drag force with swarm correction, virtual mass force, transversal lift force, and the turbulent dispersion force. A detailed explanation of these forces is not given in this paper however more details can be found at Yamoah et al. [4].

2.5 Meshing and Simulation

The rectangular test channel is replicated and meshed using Salome software then the exported mesh is transferred to OpenFOAM-V8 with the help of *ideasUnvToFoam* utility that can be found in the $FOAM_UTILITIES directory. Pure hexahedron meshes are used to mesh the inlet, outlet patches with walls, and internal meshes. In total, 187,518 elements

were used to mesh the whole test section. The inlet boundary is placed at the center of the channel as a square patch. For convivence in meshing, the cylindrical nozzle is converted into a square one by keeping the total cross-sectional area constant. Starting from the inlet the meshes expanded with a scale ratio of 0.5. A fixed local length of 0.025 m is used for a single cell in the vertical direction. The meshing can be seen in Fig. 4.

After the meshing is done and imported to OpenFOAM, the *setFieldsDict* utility is used to set the initial conditions in the test section. The simulations were performed in parallel on distributed processors using Message Passing Interface (MPI) standard. In total, 16 processors were used and the decomposition was performed using the *decomposeParDict* with *scotch* decomposition method which does not require a geometric input from the user and automatically minimizes the number of boundaries between the processors. All simulations were run for 10 seconds with a maximum Courant number less than 0.6. The main solver is using the PIMPLE algorithm where the momentum equation is first solved using an initial guess for pressure and then the pressure equation is solved three times using the velocity obtained from the momentum equation in the previous step. Before the end of the main loop, a pressure correction loop applies the updated velocity based on the updated pressure. This is repeats until convergence at each time step. More details can be found in the related OpenFOAM documentation and the literature.

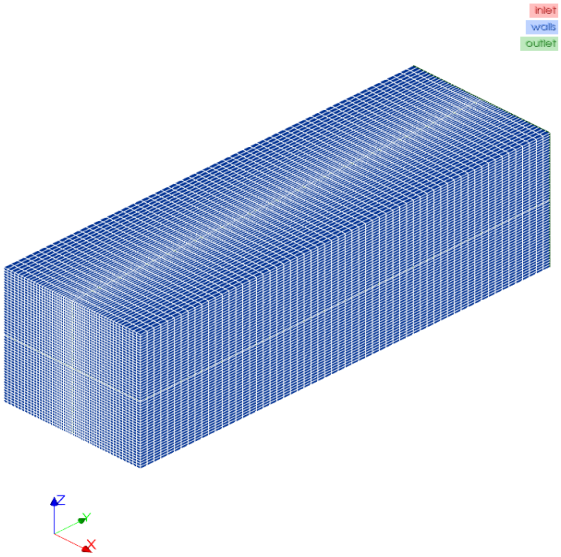

Fig. 4. Overall mesh of the test section

2.6 Results

The analyses were performed using the constant diameter model in OpenFOAM assuming a 6 mm bubble size with *mixtureKEpsilon* turbulence model. The void fraction and gas velocity results are provided by Y. Abe et. al. [2] as shown in Fig. 2 which are also the main parameters to investigate in this analysis. The importance of interfacial forces is introduced in Section 2.3 and Drag and Virtual Mass forces are included in the simulations. The drag force is unarguably the most important force acting on bubbles which control the rise velocity through the water. The virtual mass force is also very important for a stable swarm formation since it is related to the acceleration of the continuous phase relative to the dispersed one.

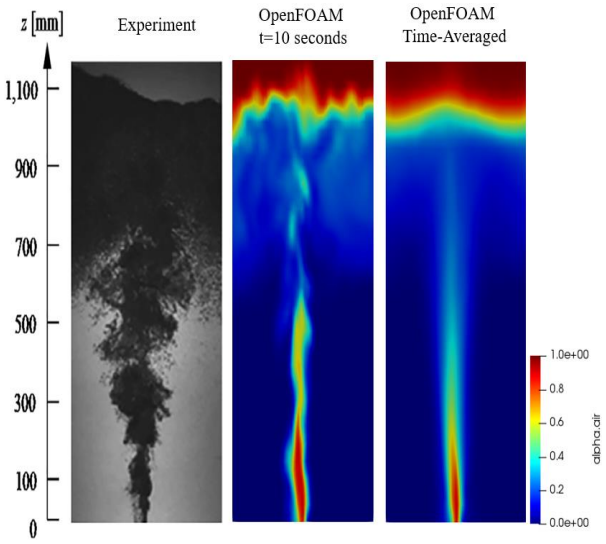

Fig. 5. Void fraction comparison

The void fraction comparison in Fig. 5. shows similar results, especially in the swarm area. However, the swarm radius toward the upstream does not seem to be gradually increasing as it is shown in the experiment, unlike the time-averaged results.

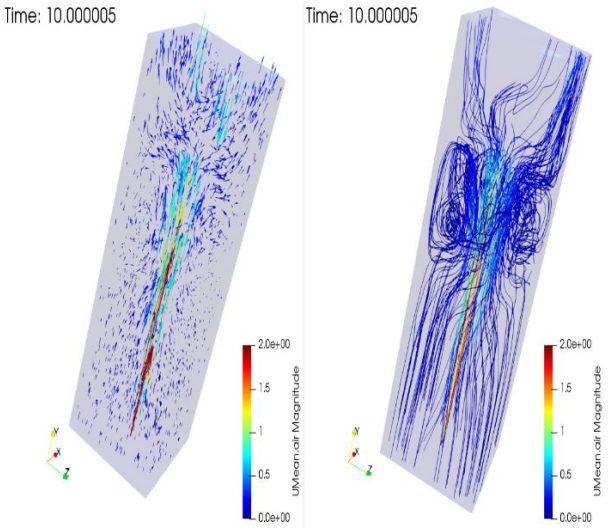

Fig. 6. Vector plot and streamlines

The high inlet air velocity does not seem to be reduced enough to transit to swarm regime at lower elevations which is the expected behavior observed in pool scrubbing experiments. The recirculation flow near the

walls is visible in both vector and streamline plots as shown in Fig. 6. To further investigate the results, the void fraction and gas velocity comparisons at each elevation are given in Figures 7 and 8.

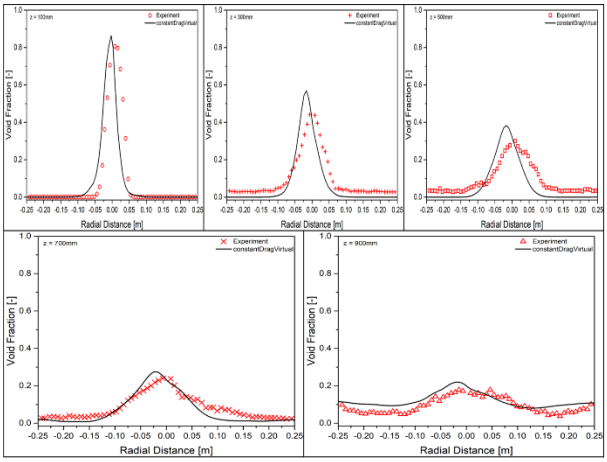

Fig. 7. The void fraction at each elevation

The void fraction results reasonably agree with the experiment results as can be seen in Figure 7. The sharp void fraction profile flattens toward downstream which is the expected behavior in the transition from globule to swarm region at pool scrubbing experiments.

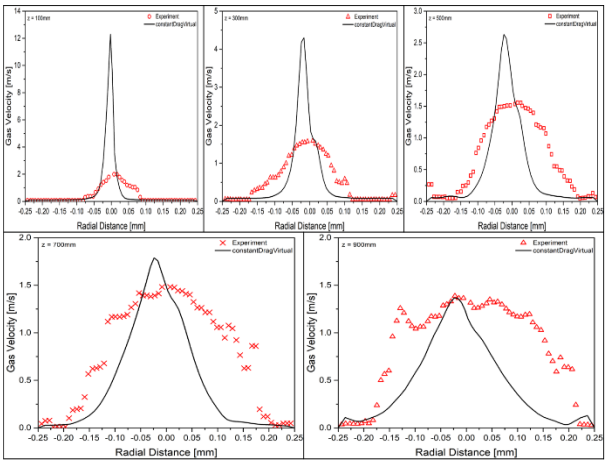

Fig. 8. Gas velocity at each elevation

The gas velocity results given in Fig. 8 show a large discrepancy near the exit and the order of the discrepancy gets smaller toward downstream. The inlet velocity of 150 m/s is quite large compared to other pool scrubbing experiments in the literature, so it is harder to evaluate an accurate gas velocity accurately. Other factors contributed to such high differences near the exit which are more elaborated in the conclusion section.

3. Conclusions

High inlet velocity airflow into a large tank is simulated using OpenFOAM. The modeling of high inlet velocity experiments using CFD is rather challenging considering the many factors that can contribute to discrepancies in the results.

One should be careful in modeling the interphase momentum exchange terms which directly affect the bubble size, shape, and velocity. In this simulation, only the drag and virtual mass forces were used. Given the differences between the simulation and experiment results, other important forces such as lift and turbulent dispersion should also be activated and the effects of all forces should be carefully investigated on the parameters. It should also be remembered that these forces are mainly correlations that come from empirical data so it is required to do extensive sensitivity and parametric tests to obtain the optimum coefficients that are factored in these interfacial forces.

It is important to note that the experiment was performed with a wire mesh sensor which could also contribute to the error in the experiment in different ways. For example, when the relative gas velocity is low the bubbles could get trapped by the wire which can cause discrepancies in void fraction estimation. Another factor could be the downward flow due to internal circulation since the wire mesh sensor is not capable of measuring negative velocities.

To further improve the results, it is intended to improve the turbulence modeling while using the constant diameter model. Once the turbulence modeling is matured and all the necessary phase interaction models are included, the diameter model should be switched to Interfacial Area Transport Equation (IATE) to get a better bubble size distribution which is crucially important when calculating the decontamination factors in pool scrubbing codes. The authors are intended to improve the bubble interaction mechanisms in OpenFOAM which are currently limited to random collision and wake entrainment in bubble coalesce and turbulent break-up in bubble disintegration. After reflecting on all the improvements, the bubble size, shape, and velocity should follow suit and a better bubble size distribution can also improve the results of the pool scrubbing codes.

REFERENCES

[1] Tokyo Electric Power Company, Inc, The 4th Progress Report on the Investigation and Examination of Unconfirmed and Unresolved Issues on the Development Mechanism of the Fukushima Daiichi Nuclear Accident, Press Release, p. 6, 2015.
[2] Y. Abe, K. Fujiwarab, S. Saitob, T. Yuasab, A. Kaneko. Bubble dynamics with aerosol during pool scrubbing, Nucl. Eng. Des., pp. 96-107, 337 (2018).
[3] P. C. Owczarski and K. W. Burk, SPARC-90: a Code for Calculating Fission Product Capture in Suppression Pools, NUREG/CR-5765, 1991.
[4] Yamoah, S., Martínez-Cuenca, R., Monrós, G., Chiva, S. and Macián-Juan, R.,Numerical Investigation of Models for Drag, Lift, Wall Lubrication and Turbulent Dispersion Forces for the Simulation of Gas-Liquid Two-Phase Flow. Chemical Engineering Research and Design, 98, 17-35, 2015.